STATIC AND DYNAMIC RESPONSE OF LAMINATED MAGNETOELECTROELASTIC BEAMS AND PLATES

by

Paul Heyliger and Fernando Ramirez
Department of Civil Engineering
Colorado State University
Fort Collins, CO 80523

Ernian Pan
Department of Mechanical Engineering
University of Akron
Akron
OH

ABSTRACT

The two-dimensional behavior of laminated magnetoelectroelastic laminates is investigated for simply supported plates under conditions of cylindrical bending. These laminates are composed of a collection of elastic, piezoelectric, and magnetostrictive layers with perfect bonding between each interface, and are subjected to specific surface tractions and/or combinations of electric or magnetic potentials. We investigate the through-thickness behavior of the five primary unknowns (the three displacements and the electric and magnetic potentials) for the case of static applied traction and potentials. Results are compared with exact solutions for the case of cylindrical bending and excellent agreement is found. Applied electrostatic potential and magnetic potential are considered to assess the level of actuation and sensing that is possible in this novel materials. The free vibration behavior is also studied. Natural frequencies and through thickness modal distribution are computed for the traction free laminate, and several notable features of the response spectrum are presented. [1]

INTRODUCTION

Magnetoelectroelastic laminates possess coupled field behavior between the elastic, electric, and magnetic field variables that depend strongly on the specific edge and surface conditions and the combination of the material parameters within the different layers. These laminates can contain three different types of materials: 1) elastic materials that possess physical relations between stress and strain fields and electric displacement and electric fields, but no coupling between the elastic and electric fields nor the elastic and magnetic fields; 2) piezoelectric materials that possess the same couplings as elastic materials but also possess coupling between the electric and elastic fields; and 3) magnetostrictive materials that possess the same couplings as elastic materials but also possess coupling between the magnetic and elastic fields. Problems involving coupled magnetoelectroelastic media have been considered by Harshe [3], Nan [4], and Benveniste [5]. The three-dimensional behavior of magnetoelectroelastic laminates under simple support has

[1] Paul Heyliger and Fernando Ramirez - Department of Civil Engineering - Colorado State University - Fort Collins, CO 80523, and Ernian Pan - Department of Mechanical Engineering - University of Akron - Akron, OH

been studied by Pan [6], and Pan and Heyliger [7]. More general static response has been considered by Pan [6] and heyliger [11].

THEORY

Geometry and Governing Equations

We consider a laminated solid that is either very thin or infinitely long in the y-direction and composed of an arbitrary number of elastic, piezoelectric, or magnetostrictive layers. The laminate has dimensions L_x in the x-direction and has total thickness H, with individual layer thicknesses of H_1, H_2, and so on labeled from the bottom up. Each layer has the constitutive equations that can be expressed as [3]:

$$\begin{aligned} \sigma_i &= C_{ik}\gamma_k - e_{ki}E_k - q_{ki}H_k \\ D_i &= e_{ik}\gamma_k + \epsilon_{ik}E_k + d_{ik}H_k \\ B_i &= q_{ik}\gamma_k + d_{ik}E_k + \mu_{ik}H_k \end{aligned} \tag{1}$$

Here C_{ij}, ϵ_{ij}, and μ_{ij} are the components of elastic stiffness, dielectric and magnetic permittivity, respectively. The symbols σ_i, D_i, and B_i denote the components of stress, electric displacement, and magnetic flux, and γ_k, E_k, and H_k denote the components of linear strain, electric field, and magnetic field, respectively. The standard contraction in indices has been used here for the elastic variables (i.e. γ_4=γ_{23}, etc.).

The components of strain, electric field, and magnetic field are related to the displacement field u_i, and the electric and magnetic potentials ϕ and ψ by the relations

$$\gamma_{ij} = \frac{1}{2}\left(\frac{\partial u_i}{\partial x_j} + \frac{\partial u_j}{\partial x_i}\right) \tag{2}$$

$$E_i = -\phi_{,i} \tag{3}$$

$$H_i = -\psi_{,i} \tag{4}$$

Within the laminate, the body force vector f_i and the free charge density ρ_f are known functions of position. Under these conditions, the equations of equilibrium and the Gauss's laws for electrostatics and magnetism are given as

$$\sigma_{ij,j} + f_i = \rho u_{i,tt} \tag{5}$$

$$D_{i,i} = \rho_f \tag{6}$$

$$B_{i,i} = 0 \tag{7}$$

We seek approximate solutions to this system of equations using the Ritz method combined with approximating functions that allow for breaks in the gradients of the three displacement components and the two potentials across a dissimilar material interface.

Variational Formulation

Following a formulation that is standard in variational methods of approximation (see Reddy [8]), we multiply the equations of equilibrium, Gauss's law, and Gauss's law for

magnetism by arbitrary functions that physically represent a virtual displacement δu_i, a virtual electrostatic potential $\delta\phi$, and a virtual magnetic potential $\delta\psi$, respectively. We then integrate the result over the volume of our domain and set the result equal to zero. This results in

$$\int_V \delta u_i(\sigma_{ij,j} + f_i - \rho u_{i,tt})dV = 0 \tag{8}$$

$$\int_V \delta\phi(D_{i,i} - \rho_f)dV = 0 \tag{9}$$

$$\int_V \delta\psi(B_{i,i})dV = 0 \tag{10}$$

Integrating these equations by parts and applying the divergence theorem yields the final weak form of our governing equations. For example, the charge equation becomes

$$\begin{aligned} 0 = \int_V \Bigg\{ &\left[e_{11}\frac{\partial u}{\partial x} + e_{14}\frac{\partial v}{\partial z} + e_{15}\left(\frac{\partial u}{\partial z} + \frac{\partial w}{\partial x}\right) + e_{16}\frac{\partial v}{\partial x} - \epsilon_{11}\frac{\partial \phi}{\partial x} - d_{11}\frac{\partial \psi}{\partial x}\right]\frac{\partial \delta\phi}{\partial x} \\ &\left[e_{21}\frac{\partial u}{\partial x} + e_{24}\frac{\partial v}{\partial z} + e_{25}\left(\frac{\partial u}{\partial z} + \frac{\partial w}{\partial x}\right) + e_{26}\frac{\partial v}{\partial x} - \epsilon_{12}\frac{\partial \phi}{\partial x} - d_{12}\frac{\partial \psi}{\partial x}\right]\frac{\partial \delta\phi}{\partial y} \\ &\left[e_{31}\frac{\partial u}{\partial x} + e_{33}\frac{\partial w}{\partial z} + e_{36}\frac{\partial v}{\partial x} - \epsilon_{33}\frac{\partial \phi}{\partial z} - d_{33}\frac{\partial \psi}{\partial z}\right]\frac{\partial \delta\phi}{\partial z} - \rho_f\delta\phi\Bigg\} dV - \oint_S D_j n_j \delta\phi dS \end{aligned} \tag{11}$$

Discrete-Layer Approximation

Approximations to the three displacements, electrostatic potential, and magnetic potential are generated in terms of the global (x,y,z) coordinates. In this study, the dependence of the displacements on the z coordinate is separated from the functions in x and y. This allows for global functions in x and y that result in a subsequent reduction of the size of the computational problem. Additionally, the laminates are considered infinitely long in the y-direction, eliminating the dependence of the approximations on the y coordinate. Hence approximations for the five unknown field quantities are sought in the form (see [8])

$$u(x,z,t) \quad = \quad \sum_{j=1}^{n} U_j(x)\Gamma_j^u(z) = \sum_{i=1}^{m}\sum_{j=1}^{n} U_{ji}\Gamma_i^u(x)\Gamma_j^u(z)\Gamma^t(t) \tag{12}$$

The approximations for each of the five field quantities are constructed in such a way as to separate the dependence in the plane with that in the direction perpendicular to the interface. The reason for this is that the change in the material properties forces a break in the gradients of the displacements across an interface. This can be easily seen by considering the specialized case of elastostatic and electrostatics. In the former case, the shear stress must be continuous across an interface, but the shear modulus is different for two layers. Hence the shear strain must be different, implying changes in the slope of the displacement variables across the interface. Similar behavior is true in electrostatics since the electric displacement must be continuous and the dielectric constants are different.

In the thickness direction, one-dimensional Lagrangian interpolation polynomials are used for $\Gamma_j(z)$ for each of the five variables. For the in-plane approximations (i.e. that in

the x-direction), different types of approximations can be used for the one-dimensional functions $\Gamma_j(x)$. Power and Fourier series are those most commonly selected. For a laminate with n layers, (n-1) is the number of subdivisions through the parallelepiped thickness (typically taken equal to or greater than the number of layers in the parallelepiped), and U_{ji}, V_{ji}, W_{ji}, Φ_{ji}, and Ψ_{ji} are the values of the respective component at height j corresponding to the i-th in-plane approximation function [10].

Substituting these approximations into the weak form and collecting the coefficients of the variations of the displacements allows one to place the results in standard matrix form [8].

$$[M]\{\ddot{u}\} + [K]\{u\} = \{f\} \tag{13}$$

For static analysis, the inertial effects are ignored. Therefore, the governing matrix equation can be expressed in simplified form as

$$[K]\{u\} = \{f\} \tag{14}$$

The dynamic analysis of the laminates is developed by using equation 13. The natural frequencies and the corresponding modal functions for traction-free vibration can be found using the assumptions of periodic motion, yielding

$$\left([\bar{K}] - \omega^2[M]\right)\{\Delta\} = \{0\} \tag{15}$$

where $[\bar{K}]$ is the condensed stiffness matrix, Δ represents the modes shapes, and ω is the natural frequency.

NUMERICAL EXAMPLES AND DISCUSSION

The primary focus of this study is to introduce the enclosed approximate model as an alternative to the far more cumbersome and restrictive exact solution approach. Exact solutions, while being extremely valuable, are limited to very specific sets of plate boundary conditions. Two different materials are studied in the examples that follow. The first is the much-studied piezoelectric solid $BaTiO_3$, the second is the purely magnetostrictive material $CoFe_2O_4$. The material properties for all of these solids are given in Table 1 along with the appropriate units for each. All the problems considered here model a plate with dimensions of $L_x = 0.01m$ and $H = 0.001m$. The edge boundary conditions are restricted to be consistent with those of geometric simple support; the transverse displacement w is specified to be zero, with zero normal traction also specified along the edge length. In terms of the electric and magnetic field variables, they are zero along the edges, but non-zero fields can be specified along the top and bottom surfaces of the laminate.

The in-plane approximation functions for each of the five field variables are given in the form of a single trigonometric series term, with the functions $\Gamma(x)$ in u and v being cos px and w, ϕ, and ψ being sin px, where $p = np/L_x$. Here the index j is a single integer that is linked to the numbers used for p in each of the terms. For all the loadings considered here, only a single term needs to be used to match the exact solution, as the fields with $n = 1$ identically satisfy the (x) dependence of all five field variables in equations (5)-(7).

Static Response

Two examples are presented here: a two-layer $BaTiO_3/CoFe_2O_4$ composite laminate under applied traction, and three-layer $BaTiO_3/CoFe_2O_4/BaTiO_3$ composite laminate under applied electrostatic and magnetic potentials. For all the examples equal layer thicknesses are used for each lamina.

Two-Layer $BaTiO_3/CoFe_2O_4$ Composite Laminate

The first example considered here have been studied using an exact approach by Pan and Heyliger [7]. Results are in excellent agreement with these problems. The loading is a positive normal traction in the positive z direction on the upper face of the laminate that has the form:

$$t_z = \sin\left(\frac{\pi x}{L_x}\right) \tag{16}$$

All other tractions on the top and bottom surfaces of the laminate are zero, as well as the specified electric displacement and magnetic flux. The plate is divided into a sequentially higher number of layers starting with 2, then 4, 8, 16, and finally 32. Results for u, w, ϕ, and ψ are shown in table 2 as a function of thickness position and number of discrete layers. The values shown are the maximum quantities at the edges of the plate for u, and at the plate center for w, ϕ, and ψ. It is clear that even for a fairly small number of layers (i.e. 4), the present results are well within 5 percent error of the exact solution values.

Three-Layer $BaTiO_3/CoFe_2O_4/BaTiO_3$ Composite Laminates

For these examples the three-layer laminates are divided into a number of layers starting with 6, then 12, 24, and finally 48. The laminate is analyzed first under applied electrostatic potential, and then under applied magnetic potential, having both applied potentials the same form of equation 16. All the other tractions are zero. Results for u, w, ϕ, and ψ are shown in Figure 1 for the case of applied electrostatic potential and in Figure 2 for the case of applied magnetic potential. The stress and electric/magnetic flux thickness distributions are shown in Tables 3 and 4.

Dynamic Response: Simple Support

Free vibrations of the three-layer composite laminate are studied in this example using a 48-layer discretization. Two cases are studied. First the purely elastic material (no coupling between elastic, electric, and magnetic fields) is analyzed, and then the magnetoelectroelastic laminate is considered by including the coupling terms. All tractions are zero, and the magnetic and electrostatic potentials are specified to zero along the top and bottom surfaces of the laminate. Frequencies and mode shapes are calculated only for the first axial mode (i.e. $p = \pi/L_x$). For this mode, only the first thirty thickness modes are presented here. Natural frequencies in radians per second are shown in Table 5. Surprisingly, many of the modes from the fully coupled analysis are either purely elastic (E: no influence of e_{ij} or q_{ij}) or piezoelectric (P: no influence of q_{ij}), but none are purely magnetostrictive within the first 147 modes computed.

Parameter	$CoFeO_4$	$BaTiO_3$
C_{11} (Gpa)	286.0	166.0
C_{22}	286.0	166.0
C_{33}	269.5	162.0
C_{13}	170.5	78.0
C_{23}	170.5	78.0
C_{12}	173.0	77.0
C_{44}	45.3	43.0
C_{55}	45.3	43.0
C_{66}	56.5	44.5
e_{31} (C/m^2)	0.0	-4.4
e_{32}	0.0	-4.4
e_{33}	0.0	18.6
e_{24}	0.0	11.6
e_{15}	0.0	11.6
q_{31} (N/Am)	580.3	0.0
q_{32}	580.3	0.0
q_{33}	699.7	0.0
q_{24}	550.0	0.0
q_{15}	550.0	0.0
ϵ_{11} $(10^{-9}C^2/Nm^2)$	0.080	11.2
ϵ_{22}	0.080	11.2
ϵ_{33}	0.093	12.6
$d_{11} = d_{22} = d_{33}$	0.0	0.0
μ_{11} $(10^{-6}Ns^2/C^22)$	-590.0	5.0
μ_{22}	-590.0	5.0
μ_{33}	157.0	10.0

Table 1: Material properties and units for the two materials used in numerical examples.

z (m)	0.0000	0.0005	0.0010
N=2	1.0436	-0.0576	-1.1720
N=4	1.1267	-0.0634	-1.2636
N=8	1.1420	-0.0650	-1.2891
N=16	1.1558	-0.0654	-1.2957
N=32	1.1573	-0.0655	-1.2973
Exact	1.1578	-0.0655	-1.2979

a. In-Plane displacement $u(10^{-12}m.)$.

z (m)	0.0000	0.0005	0.0010
N=2	7.2310	7.2807	7.2463
N=4	7.7784	7.8316	7.7946
N=8	7.9309	7.9850	7.9473
N=16	7.9701	8.0244	7.9865
N=32	7.9799	8.0344	7.9964
Exact	7.9832	8.0377	7.9997

b. Transverse displacement $w(10^{-12}m.)$.

z (m)	0.0000	0.0005	0.0010
N=2	2.1346	2.1574	1.3134
N=4	2.1389	2.1616	1.2500
N=8	2.1404	2.1632	1.2327
N=16	2.1408	2.1636	1.2283
N=32	2.1409	2.1637	1.2272
Exact	2.1410	2.1637	1.2268

c. Electrostatic Scalar Potential $\phi(10^{-4}V)$.

z (m)	0.0000	0.0005	0.0010
N=2	-1.9834	-2.6335	-2.6173
N=4	-1.7744	-2.4631	-2.4479
N=8	-1.7172	-2.4166	-2.4018
N=16	-1.7026	-2.4048	-2.3900
N=32	-1.6989	-2.4018	-2.3870
Exact	-1.6977	-2.4008	-2.3860

d. Magnetic Vector Potential $\psi(10^{-7}C/s)$.

Table 2: Maximum displacements and potential for the two-layer laminate $BaTiO_3/CoFe_2O_4$ under transverse load.

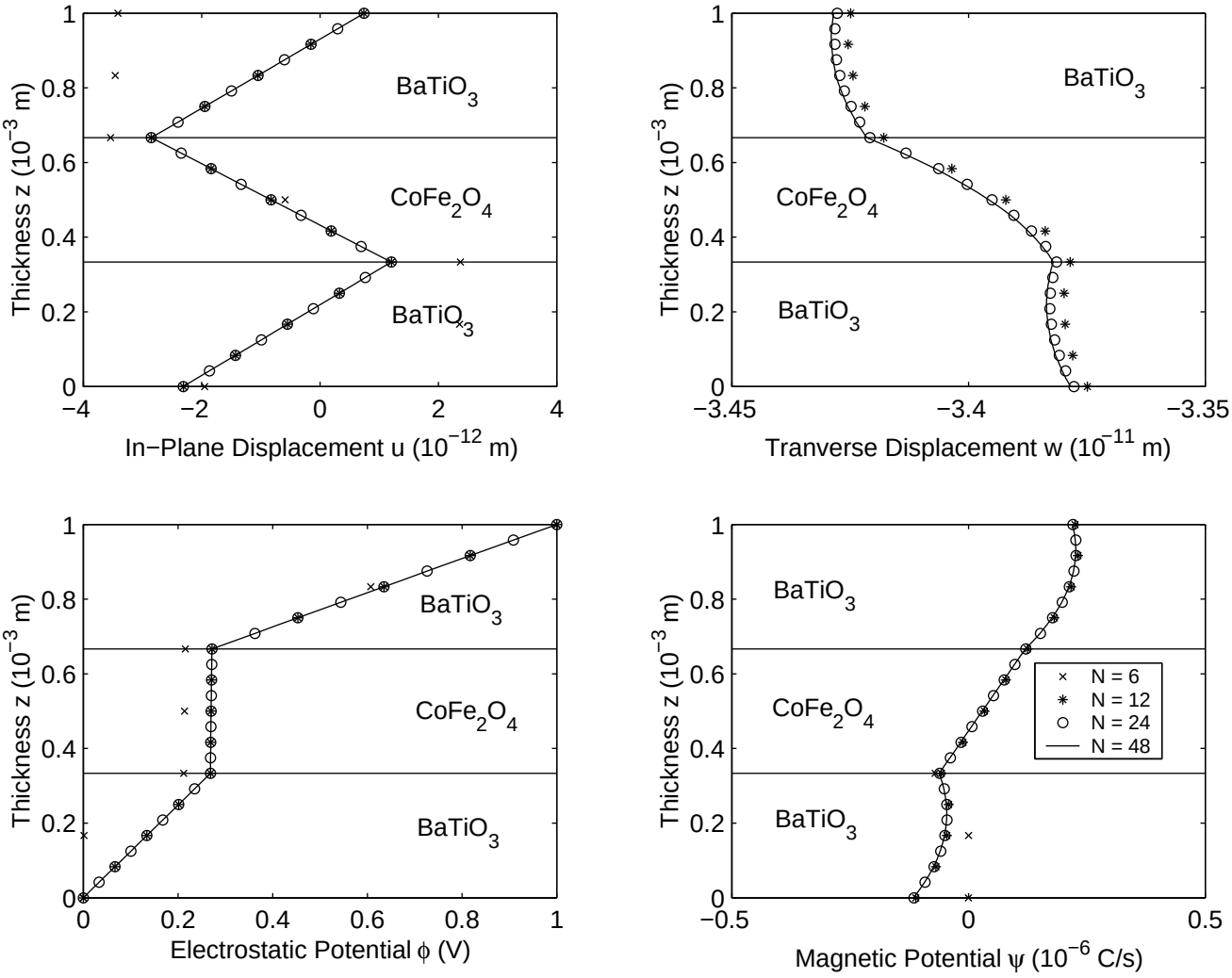

Figure 1: Variation of displacement components, electrostatic and magnetic potential through the laminate thickness for the 3-layer $BaTiO_3/CoFe_2O_4/BaTiO_3/$ laminate under applied electrostatic potential.

$z(10^{-3}m)$	$\sigma_{xx}(Pa)$	$\sigma_{zz}(Pa)$	$\sigma_{xz}(Pa)$	$D_{zz}(C/m^2)$	B_{zz} (N/Am)
4.16667E-05	1.04440E+02	-1.92100E-02	-1.53990E+00	-7.48740E-08	-4.66390E-10
1.25000E-04	5.51490E+01	-8.73070E-02	-3.62830E+00	-7.49180E-08	-1.63900E-09
2.08333E-04	5.95510E+00	-1.93210E-01	-4.42790E+00	-7.50060E-08	-3.15950E-09
2.91667E-04	-4.32280E+01	-3.03190E-01	-3.94020E+00	-7.51390E-08	-4.71120E-09
3.75000E-04	-1.13520E+02	-3.78010E-01	-1.60050E+00	-9.10740E-08	-5.45680E-09
4.58333E-04	-9.74100E+01	-3.84100E-01	1.16030E+00	-1.22820E-07	-5.45630E-09
5.41667E-04	-8.14300E+01	-3.23420E-01	3.50110E+00	-1.54620E-07	-5.45770E-09
6.25000E-04	-6.55570E+01	-2.06920E-01	5.42510E+00	-1.86510E-07	-5.46100E-09
7.08333E-04	1.34370E+02	-7.56040E-02	4.23200E+00	-2.02600E-07	-4.43150E-09
7.91667E-04	8.39700E+01	-2.66880E-03	1.37480E+00	-2.02890E-07	-2.69280E-09
8.75000E-04	3.37220E+01	1.27080E-02	-1.65290E-01	-2.03310E-07	-1.48290E-09
9.58333E-04	-1.64640E+01	4.97040E-03	-3.91130E-01	-2.03850E-07	-4.84100E-10

Table 3: Variation of stress components, electrostatic displacement, and magnetic flux through the laminate thickness for 3-layer $BaTiO_3/CoFe_2O_4/BaTiO_3/$ laminate under applied electrostatic potential.

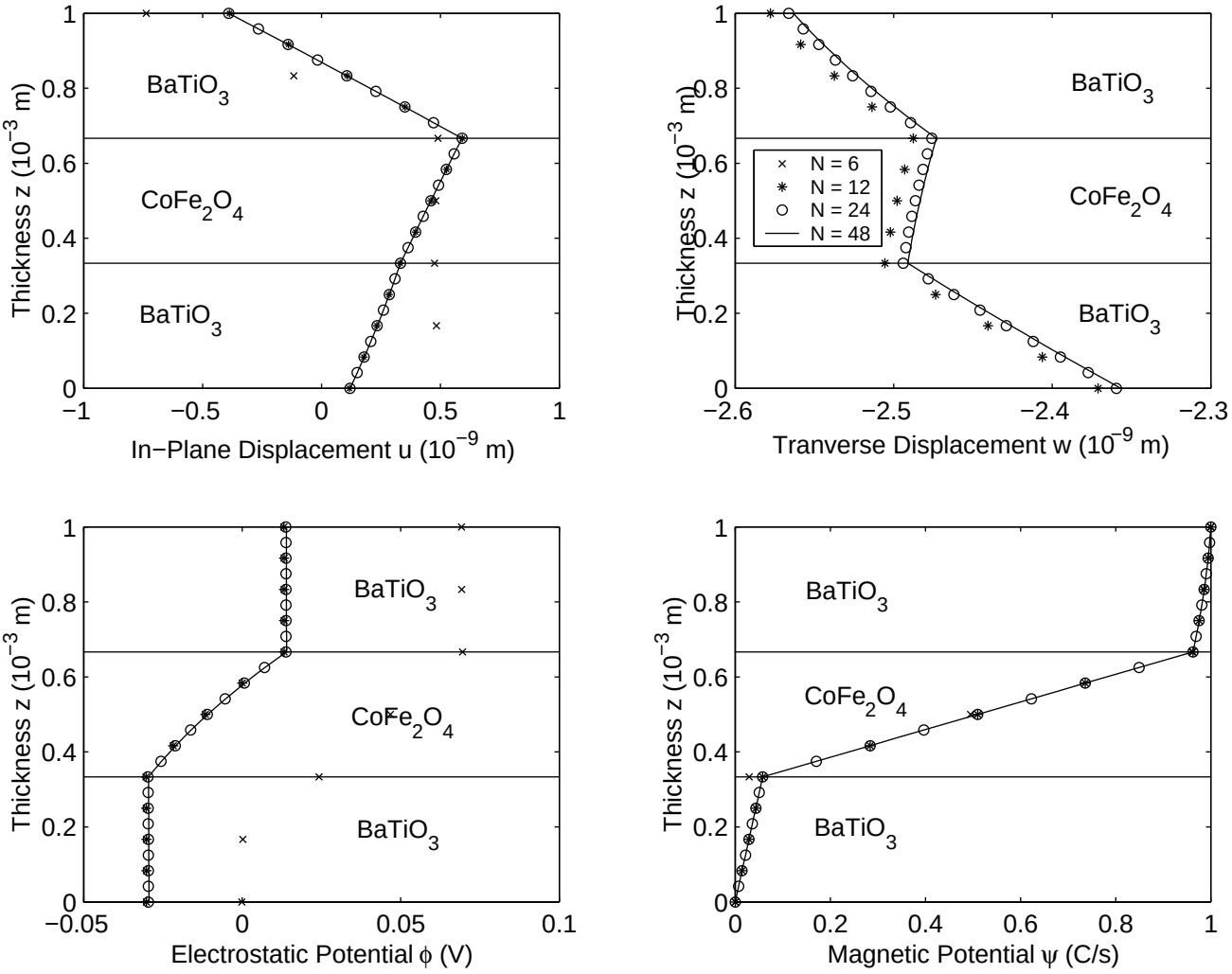

Figure 2: Variation of displacement components, electrostatic and magnetic potential through the laminate thickness for the 3-layer $BaTiO_3/CoFe_2O_4/BaTiO_3/$ laminate under applied magnetic potential.

$z(10^{-3}m)$	$\sigma_{xx}(Pa)$	$\sigma_{zz}(Pa)$	$\sigma_{xz}(Pa)$	$D_{zz}(C/m^2)$	B_{zz} (N/Am)
4.16667E-05	1.56780E+04	-7.21630E+00	-2.16950E+02	9.92780E-12	-2.76620E-02
1.25000E-04	1.23830E+04	-1.77120E+01	-5.83420E+02	2.97890E-11	-2.75920E-02
2.08333E-04	9.26370E+03	-3.66890E+01	-8.65950E+02	4.96680E-11	-2.74530E-02
2.91667E-04	6.31290E+03	-6.20100E+01	-1.06900E+03	6.95770E-11	-2.72460E-02
3.75000E-04	-1.60940E+04	-8.40760E+01	-9.39040E+02	-1.66530E-09	-2.71220E-02
4.58333E-04	-1.89410E+04	-1.02690E+02	-4.80520E+02	-4.15530E-09	-2.71330E-02
5.41667E-04	-2.18160E+04	-1.08320E+02	5.28970E+01	-4.33470E-09	-2.71540E-02
6.25000E-04	-2.47220E+04	-9.89920E+01	6.61970E+02	-1.85370E-09	-2.71850E-02
7.08333E-04	-4.91600E+03	-7.97080E+01	1.10460E+03	3.04000E-11	-2.48830E-02
7.91667E-04	4.60520E+03	-4.98770E+01	1.10930E+03	2.17010E-11	-2.02040E-02
8.75000E-04	1.42470E+04	-2.31990E+01	8.63110E+02	1.30160E-11	-1.54740E-02
9.58333E-04	2.40000E+04	-6.28240E+00	3.62970E+02	4.33770E-12	-1.07050E-02

Table 4: Variation of stress components, electrostatic displacement, and magnetic flux through the laminate thickness for 3-layer $BaTiO_3/CoFe_2O_4/BaTiO_3/$ laminate under applied magnetic potential.

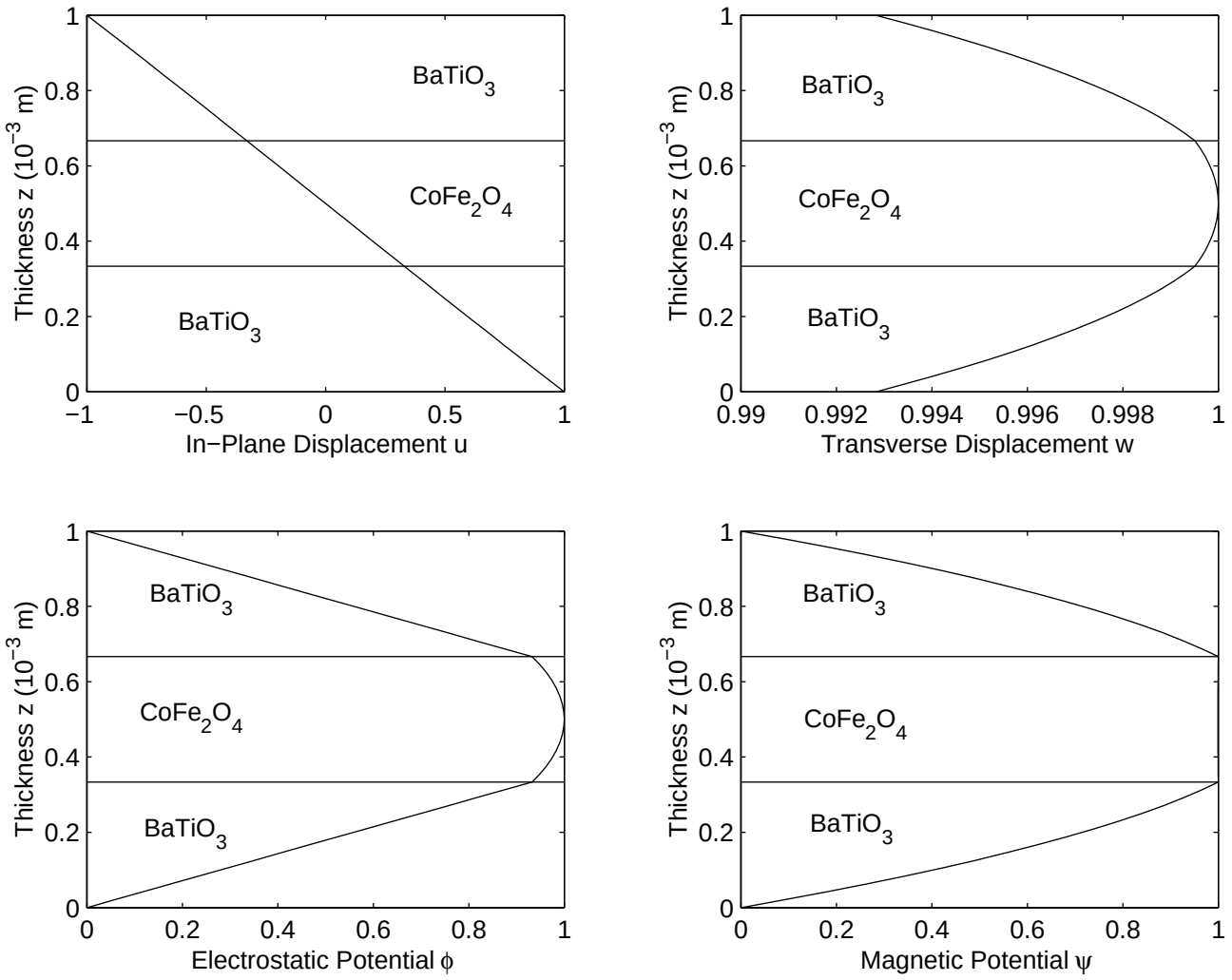

Figure 3: Through thickness mode shapes for the 3-layer $BaTiO_3/CoFe_2O_4/BaTiO_3$ laminate.

N	Coupled	T	Uncoupled	N	Coupled	T	Uncoupled	N	Coupled	T	Uncoupled
1	117.3		117.0	11	26548.6	E	26548.6	21	53684.9	E	53684.9
2	719.8	E	719.8	12	26553.9		26552.8	22	53688.4	P	53687.5
3	1277.0		1260.8	13	31447.0		30568.1	23	60534.4	P	58497.7
4	6622.9	E	6622.9	14	33343.3	E	33343.3	24	60602.0		60534.4
5	6937.1		6725.6	15	33398.6		33352.5	25	60852.5		60539.8
6	13244.8		13089.6	16	40038.4	P	40036.8	26	67419.1	E	67419.1
7	13331.7	E	13331.7	17	40039.8	P	40038.4	27	67420.9	P	67420.0
8	14684.7		14022.5	18	46557.3		45338.3	28	74544.8	E	74544.8
9	19932.8	E	19932.8	19	46757.5	E	46757.5	29	74561.3	P	74546.2
10	20219.6		19933.5	20	46798.5		46759.2	30	77629.0		74893.5

Table 5: Frequencies ω x 10^{-5} for the 3-layer $BaTiO_3/CoFe_2O_4/BaTiO_3$ laminate.

References

[1] Saravanos, D. A., and Heyliger, P. R., "Mechanics and Computational Models for Laminated Piezoelectric Beams, Plates, and Shells, Appl. Mech. Rev., Vol. 52, pp. 305-320 (1999).

[2] Tzou, H.S., Piezoelectric Shells: Distributed Sensing and Control of Continua, Kluwer Academic, Norwell, MA (1993).

[3] Harshe, G., Dougherty, J. P., and Newnham, R. E., "Theoretical Modeling of Multilayer Magneoelectric Composites, Int. J. Appl. Electromag., Vol. 4, pp. 145-159 (1993).

[4] Nan, C. W., "Magnetoelectric Effect in Composites of Piezoelectric and Piezomagnetic Phases, Phys. Rev. B, Vol. B50, pp. 6082-6088 (1994).

[5] Benveniste, Y., "Magnetoelctric Effect in Fibrous Composites with Piezoelectric and Piezomagnetic Phases, Phys. Rev. B, Vol. B51, pp. 16424-16427 (1995).

[6] Pan, E., "Exact Solution for Simply Supported and Multilayered Magneto-Electro-Elastic Plates, J. Appl. Mech., Vol. 68, pp. 608-618 (2001).

[7] Pan, E., and Heyliger, P. R., "Free Vibrations of Simply-Supported and Multilayered Magneto-Electro-Elastic Plates, J. Sound Vibr., Vol. 252, pp. 429-442 (2002).

[8] Reddy, J. N., Energy and Variational Methods in Applied Mechanics, John Wiley and Sons, New York (1984).

[9] Pauley, K. E., and Dong, S. B., "Analysis of Plane Waves in Laminated Piezoelectric Media, Wave Electronics, Vol. 1, pp. 265-285 (1976).

[10] Reddy, J. N., "A Generalization of Displacement-Based Laminate Theories, Communications in Applied Numerical Methods, Vol. 3, pp. 173-181 (1987).

[11] Heyliger, P., "Static Behavior of Laminated Elastic/Piezoelectric Plates, AIAA J., Vol. 32, pp. 2481-2484 (1994).

[12] Heyliger, P. R., and Saravanos, D. A., "Exact Free Vibration Analysis of Laminated Plates with Embedded Piezoelectric Layers, J. Acoust. Soc. Amer., Vol. 98, pp. 154701557 (1995).

[13] Heyliger, P. R., "Exact Solutions for Simply-Supported Laminated Piezoelectric Plates, J. Appl. Mech., Vol. 64, pp. 299-306 (1997).

[14] Berlincourt, D. A., Curran, D. R., and Jaffe, H., Physical Acoustics, 1, Piezoelectric and piezomagnetical materials and their function in transducers, pp. 169-270 (1964).

[15] Robbins, D. H., and Reddy, J. N., "Variable Kinematic Modelling of Laminated Composite Plates, Int. J. Num. Meth. Engr., Vol. 39, pp. 2283-2317 (1996).

[16] Tiersten, H. F., *Linear Piezoelectric Plate Vibrations*, Plenum Press, New York (1969).

[17] Tashiro, K., Tadokoro, H., and Kobayashi, M., "Structure and Piezoelectricity of Poly(Vinylidene Flouride)", *Ferroelectrics* **32**, 167-175 (1981).

ACKNOWLEDGEMENT

PRH gratefully acknowledges the support of the Alexander von Humboldt Foundation, which sponsored the completion of this work and made travel to this conference possible.